

This is a repository copy of *Toward the limit of nuclear binding on the N=Z line: Spectroscopy of Cd 96*.

White Rose Research Online URL for this paper:

<https://eprints.whiterose.ac.uk/144021/>

Version: Published Version

---

**Article:**

Davies, P. J. [orcid.org/0000-0002-9003-0603](https://orcid.org/0000-0002-9003-0603), Park, J., Grawe, H. et al. (77 more authors) (2019) *Toward the limit of nuclear binding on the N=Z line: Spectroscopy of Cd 96*. *Physical Review C*. 021302. ISSN 2469-9993

<https://doi.org/10.1103/PhysRevC.99.021302>

---

**Reuse**

Items deposited in White Rose Research Online are protected by copyright, with all rights reserved unless indicated otherwise. They may be downloaded and/or printed for private study, or other acts as permitted by national copyright laws. The publisher or other rights holders may allow further reproduction and re-use of the full text version. This is indicated by the licence information on the White Rose Research Online record for the item.

**Takedown**

If you consider content in White Rose Research Online to be in breach of UK law, please notify us by emailing [eprints@whiterose.ac.uk](mailto:eprints@whiterose.ac.uk) including the URL of the record and the reason for the withdrawal request.

## Toward the limit of nuclear binding on the $N = Z$ line: Spectroscopy of $^{96}\text{Cd}$

P. J. Davies,<sup>1</sup> J. Park,<sup>2,3,4</sup> H. Grawe,<sup>5</sup> R. Wadsworth,<sup>1</sup> R. Gernhäuser,<sup>6</sup> R. Krücken,<sup>2,3</sup> F. Nowacki,<sup>7</sup> D. S. Ahn,<sup>8</sup> F. Ameil,<sup>5</sup> H. Baba,<sup>8</sup> T. Bäck,<sup>9</sup> B. Blank,<sup>10</sup> A. Blazhev,<sup>11</sup> P. Boutachkov,<sup>12,5</sup> F. Browne,<sup>8,13</sup> I. Čeliković,<sup>14,15</sup> M. Dewald,<sup>11</sup> P. Doornenbal,<sup>8</sup> T. Faestermann,<sup>6</sup> Y. Fang,<sup>16</sup> G. de France,<sup>14</sup> N. Fukuda,<sup>8</sup> A. Gengelbach,<sup>17</sup> J. Gerl,<sup>5</sup> J. Giovinazzo,<sup>10</sup> S. Go,<sup>18</sup> N. Goel,<sup>12,5</sup> M. Górska,<sup>5</sup> E. Gregor,<sup>12,5</sup> H. Hotaka,<sup>19</sup> S. Ilieva,<sup>12</sup> N. Inabe,<sup>8</sup> T. Isobe,<sup>8</sup> D. G. Jenkins,<sup>1</sup> J. Jolie,<sup>11</sup> H. S. Jung,<sup>18</sup> A. Jungclaus,<sup>20</sup> D. Kameda,<sup>8</sup> G. D. Kim,<sup>21</sup> Y.-K. Kim,<sup>21</sup> I. Kojouharov,<sup>5</sup> T. Kubo,<sup>8</sup> N. Kurz,<sup>5</sup> M. Lewitowicz,<sup>14</sup> G. Lorusso,<sup>8,22,23</sup> D. Lubos,<sup>6,8</sup> L. Maier,<sup>6</sup> E. Merchan,<sup>12,5</sup> K. Moschner,<sup>11,8</sup> D. Murai,<sup>8</sup> F. Naqvi,<sup>24</sup> H. Nishibata,<sup>16</sup> D. Nishimura,<sup>25</sup> S. Nishimura,<sup>8</sup> I. Nishizuka,<sup>26</sup> Z. Patel,<sup>8,23</sup> N. Pietralla,<sup>12</sup> M. M. Rajabali,<sup>2</sup> S. Rice,<sup>8,23</sup> H. Sakurai,<sup>18</sup> H. Schaffner,<sup>5</sup> Y. Shimizu,<sup>8</sup> L. F. Sinclair,<sup>1,8</sup> P.-A. Söderström,<sup>8,5</sup> K. Steiger,<sup>6</sup> T. Sumikama,<sup>26</sup> H. Suzuki,<sup>8</sup> H. Takeda,<sup>8</sup> J. Taprogge,<sup>20</sup> P. Thöle,<sup>11</sup> S. Valder,<sup>1</sup> Z. Wang,<sup>2</sup> N. Warr,<sup>11</sup> H. Watanabe,<sup>8,27</sup> V. Werner,<sup>12,24</sup> J. Wu,<sup>8,28</sup> Z. Y. Xu,<sup>8</sup> A. Yagi,<sup>29</sup> K. Yoshinaga,<sup>8</sup> and Y. Zhu<sup>30</sup>

<sup>1</sup>University of York, York YO10 5DD, United Kingdom

<sup>2</sup>TRIUMF 4004 Wesbrook Mall, Vancouver, British Columbia, V6T 2A3, Canada

<sup>3</sup>University of British Columbia, Vancouver, British Columbia, V6T 1Z1, Canada

<sup>4</sup>Department of Physics, Lund University, 22100 Lund, Sweden

<sup>5</sup>GANIL Helmholtzzentrum für Schwerionenforschung D-64291 Darmstadt, Germany

<sup>6</sup>Technische Universität München, D-85748 Garching, Germany

<sup>7</sup>Université de Strasbourg, F-67037 Strasbourg, France

<sup>8</sup>RIKEN Nishina Center, Wako-shi, Saitama 351-0198, Japan

<sup>9</sup>Royal Institute of Technology, SE-10691 Stockholm, Sweden

<sup>10</sup>Centre d'Etudes Nucléaires de Bordeaux-Gradignan, 19 Chemin du Solarium, CS 10120, F-33175 Gradignan Cedex, France

<sup>11</sup>Universität zu Köln, D-50937 Köln, Germany

<sup>12</sup>Technische Universität Darmstadt, 64289 Darmstadt, Germany

<sup>13</sup>University of Brighton, Brighton, BN2 4GJ, United Kingdom

<sup>14</sup>Grand Accélérateur National d'Ions Lourds (GANIL), CEA/DSM-CNRS/IN2P3, Boulevard H. Becquerel, 14076 Caen, France

<sup>15</sup>University of Belgrade, 11000 Belgrade, Serbia

<sup>16</sup>Osaka University, 1-1 Machikaneyama-machi, Osaka 560-0043 Toyonaka, Japan

<sup>17</sup>Uppsala University, SE-75121 Uppsala, Sweden

<sup>18</sup>University of Tokyo, Bunkyo, Tokyo 113-0033, Japan

<sup>19</sup>Department of Physics, Tokyo University of Science, Noda, Chiba 278-8510, Japan

<sup>20</sup>Instituto de Estructura de la Materia, CSIC, E-28006 Madrid, Spain

<sup>21</sup>Rare Isotope Science Project, Institute for Basic Science, Daejeon 305-811, Republic of Korea

<sup>22</sup>Acoustics and Ionizing Radiation Division, National Physical Laboratory, Teddington TW110LW, United Kingdom

<sup>23</sup>University of Surrey, Guildford GU2 7XH, United Kingdom

<sup>24</sup>Yale University, New Haven, Connecticut 06511, USA

<sup>25</sup>Tokyo City University, Setagaya-ku, Tokyo 158-8557, Japan

<sup>26</sup>Tohoku University, Sendai 980-0845, Japan

<sup>27</sup>Beihang University, Beijing 100191, China

<sup>28</sup>Peking University, Beijing 100871, China

<sup>29</sup>Osaka University, Ibaraki, Osaka 567-0047, Japan

<sup>30</sup>Tokyo University of Science, Noda, Chiba 278-8510, Japan



(Received 27 November 2017; revised manuscript received 3 August 2018; published 11 February 2019)

A  $\gamma$ -decaying isomeric state ( $\tau_{1/2} = 197_{-17}^{+19}$  ns) has been identified in  $^{96}\text{Cd}$ , which is one  $\alpha$  particle away from the last known bound  $N = Z$  nucleus,  $^{100}\text{Sn}$ . Comparison of the results with shell-model calculations has allowed a tentative experimental level scheme to be deduced and the isomer to be interpreted as a medium-spin negative-parity spin trap based on the coupling of isoscalar ( $T = 0$ ) and isovector ( $T = 1$ ) neutron-proton pairs. The data also suggest evidence for the population of a  $9^+$   $T = 1$  state, which is predicted by shell-model calculations to be yrast. Such a low-lying  $T = 1$  state, which is unknown in lighter mass even-even self-conjugate nuclei, can also be interpreted in terms of the coupling of  $T = 0$  and  $T = 1$  neutron-proton pairs.

DOI: [10.1103/PhysRevC.99.021302](https://doi.org/10.1103/PhysRevC.99.021302)

Studies of the pairing correlations between fermions has contributed greatly to our understanding of the behavior of

many-body quantum systems [1]. Nuclei contain two different types of fermions (protons and neutrons) and provide a unique

laboratory for the study of pairing since it plays a prominent role in nuclear structure physics at low excitation energies [2–9].

Isovector ( $T = 1$ ) pairing between like nucleons is the most prevalent type of pairing across the nuclear chart; in the case of the  $N = 50$  semimagic isotones below  $^{100}\text{Sn}$  (the heaviest bound  $N = Z$  nucleus [10]) this manifests as a set of nuclei that are well described by the seniority scheme [11–16]. However, in the case of self-conjugate nuclei, enhanced neutron-proton ( $np$ ) pairing correlations can arise between the two distinct fermions when they occupy the same orbitals. In addition to  $T = 1$   $np$  pairing, the opportunity for isoscalar ( $T = 0$ ) correlations is also present. Competition between these  $np$  pairing mechanisms is of contemporary interest [3, 6–8, 17–20]. While  $T = 1$   $np$  pairs have been shown to dominate the structure of  $N = Z$  nuclei below mass 80 [20, 21], evidence for a  $T = 0$   $np$  pairing condensate remains elusive.

Recent work on  $^{92}\text{Pd}$  [3] has provided the first indications at low spins for the influence of the isoscalar  $np$  interaction as well as the possibility for the existence of a new type of spin-aligned isoscalar  $np$  pair. The observation of the  $\beta$ -decaying  $16^+$  isomer in  $^{96}\text{Cd}$  [17, 22] has revealed evidence for the importance of the  $T = 0$   $np$  interaction at higher spins. These works have resulted in a number of theoretical studies that include investigations of the  $T = 0$  two-body matrix elements in a restricted shell-model space [7] and the mapping of shell-model states to a corresponding boson model [8, 19]. Such calculations indicate that the wave functions of low-lying states in  $^{96}\text{Cd}$  contain spin-aligned  $np$  pairs. However, the interpretation of excited states is often complicated by competition from isovector pairing as well as issues associated with establishing the suitability of the limited model spaces employed in shell-model calculations [18].

Due to their low production cross sections, the investigation of excited states in  $N = Z$  nuclei above mass 90 remains a challenge even for state-of-the-art experimental techniques. However, the presence of isomeric states can make such studies feasible. The nucleus  $^{96}\text{Cd}$ , which differs from  $^{100}\text{Sn}$  by just two  $np$  pairs, provides a potential laboratory for investigating the competition between  $T = 0$ ,  $T = 1$ , and spin-aligned  $np$  pair structures. Moreover, the evolution of the pair structure with increasing spin as well as the role of seniority structure, which clearly exists in  $^{98}\text{Cd}$  [13] due to the dominance of  $T = 1$  like-nucleon pairs, can be explored. The work reported in this Rapid Communication presents the first experimental evidence for  $\gamma$  rays resulting from the decay of excited states in  $^{96}\text{Cd}$ . These are observed following the population and subsequent decay of an isomeric state. In this work the new transitions are interpreted with the aid of shell-model (SM) calculations performed using different interactions and model spaces and also with other theoretical approaches. The implications for  $np$  pairing are discussed.

Excited states in  $^{96}\text{Cd}$  were produced in two independent fragmentation experiments that utilized a 345 MeV/u  $^{124}\text{Xe}$  beam, provided by the RI Beam Factory (RIBF) operated by RIKEN Nishina Center and CNS, University of Tokyo, to bombard a 740 mg/cm<sup>2</sup> thick  $^9\text{Be}$  target foil. Both experiments identified the nuclei of interest from time-of-flight and energy-loss measurements in the BigRIPS separator [23, 24]

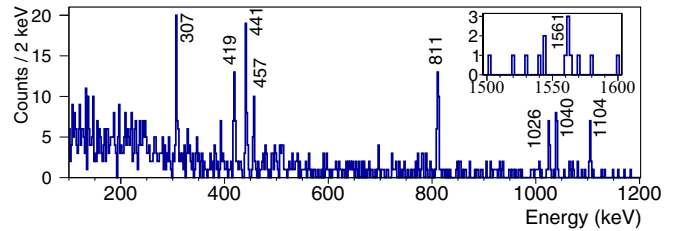


FIG. 1. Delayed  $\gamma$ -ray spectrum with detection times of 50–1200 ns after  $^{96}\text{Cd}$  implantation, summed from two independent experiments. Individual Ge crystals were used to produce the  $\gamma$ -ray events. The inset shows evidence for a weak transition at 1561 keV.

and zero degree spectrometer and implanted the nuclei in the EURICA [25] stopped beam setup. The main difference between the two experiments was the silicon active stopper (AS) in which the ions of interest were implanted. In the first experiment (RIBF83) the Silicon Implantation Beta Absorber (SIMBA) decay station [10] was employed while the Wide-range Active Silicon-Strip Stopper Array for Beta and ion detection (WAS3ABi) [26] was used in the second (RIBF9) experiment. In each case the AS was located at the center of the EURICA Ge detector array [25]. Further details concerning the particle identification are provided in Ref. [26]. Figure 1 in Ref. [22] shows the particle identification plot obtained in the RIBF83 experiment.

In the RIBF83 experiment  $\approx 17000$  ions of  $^{96}\text{Cd}$  were implanted in SIMBA over a period of  $\approx 120$  h, while for RIBF9  $\approx 18750$  ions of  $^{96}\text{Cd}$  were implanted in WAS3ABi in 203 h. However, for the latter experiment only 47 out of the 84 crystals in the EURICA Ge array were operational due to a liquid-nitrogen filling problem prior to the start of the experiment. This lowered the Ge  $\gamma$ -ray detection efficiency to 56% of EURICA’s full capacity. The  $\gamma$ -ray singles spectrum obtained from both experiments after projecting events from the time versus  $\gamma$ -ray energy matrices, within a time window of  $\approx 50$ –1200 ns, is presented in Fig. 1. This spectrum was obtained using individual Ge crystal events rather than using add-back events in the clusters due to the high  $\gamma$ -ray multiplicity.

The  $\gamma$ -ray spectrum shown in Fig. 1 reveals the presence of nine transitions that are observed between approximately 50 and 1200 ns after the implantation of  $^{96}\text{Cd}$  ions. The lower time limit was chosen to minimize the low-energy background from bremsstrahlung radiation, while the upper time limit was chosen to ensure that all events had been collected in the photopeaks of the identified  $\gamma$  rays. The relative intensities of the  $\gamma$  rays extracted from the RIBF83 experiment are presented in Fig. 4 (Exp).

To minimize any systematic error introduced by summing the data from both experiments, a separate lifetime analysis was performed for each of the data sets. In both cases time distributions between ion implantation and  $\gamma$ -ray detection were constructed by placing gates on each  $\gamma$  ray in  $\gamma$ -ray energy versus time matrices. Using the maximum likelihood method the lifetimes associated with individual transitions were obtained [28]. These are presented in the insets of Figs. 2(a) and 2(b) for experiments RIBF83 and RIBF9, respectively.

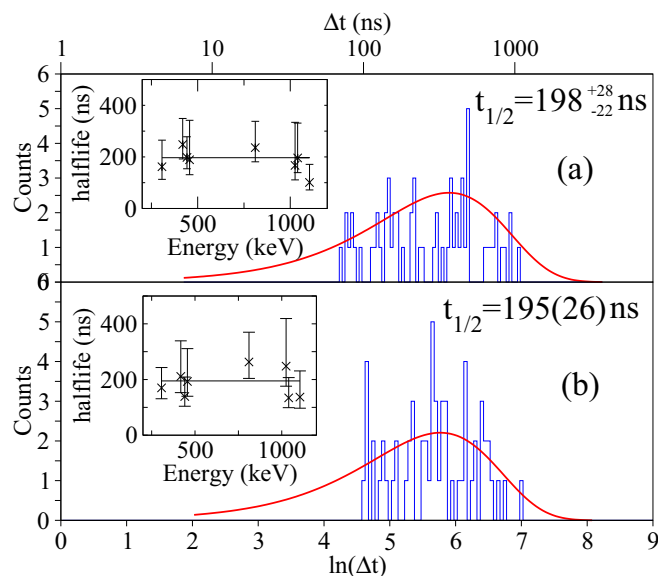


FIG. 2. Spectra showing the natural logarithm of the decay time ( $\Delta t$ , in ns, is shown on the upper axis), obtained by summing gates set on the eight main  $\gamma$  rays shown in Fig. 1 in the  $\gamma$ -ray energy vs time matrices, for experiments (a) RIBF83 and (b) RIBF9. The red line shows the best fit for the data using the Schmidt method [27] where the centroid yields the mean-lifetime. Insets show the half-lives for individual  $\gamma$  rays plotted as a function of  $\gamma$ -ray energy.

Within uncertainties, the measured lifetimes associated with individual  $\gamma$  rays of the same energy were consistent between the two experiments. Furthermore, all transitions possess the same lifetime (within errors), confirming the presence of only one long-lived isomeric state. Figures 2(a) and 2(b) show the sum of all time distributions for the eight most intense transitions from the two experiments, where  $\Delta t$  is the time between the implantation of an ion and observation of a  $\gamma$  ray. In both cases the distributions were fitted using a log-likelihood method for exponential decays with a small number of counts, known as the Schmidt method [27], the results of which yield the half-lives shown in the figure and for which the weighted average value is  $197^{+19}_{-17}$  ns. This result is consistent with the weighted average of the half-lives obtained for the individual  $\gamma$  rays, insets of Figs. 2(a) and 2(b).

Due to the nature of the experiment it is not possible to unambiguously order the observed  $\gamma$  rays. However, it is proposed that the observed transitions form a cascade from a single isomeric state. This proposal is based on the results of the lifetime analysis, the observed intensities of the  $\gamma$  rays, and results from analysis of a  $\gamma$ - $\gamma$  coincidence matrix. The  $\gamma$ - $\gamma$  data presented in Fig. 3 were obtained from the RIBF83 experiment using two coincidence conditions. The first allowed sufficient time ( $\approx 6$  half-lives) following the implantation of a  $^{96}\text{Cd}$  ion in SIMBA for the decay of the isomer, with a time window of up to 1500 ns being chosen, while the second  $\gamma$ - $\gamma$  coincidence condition used a time window of up to 200 ns. Gates were placed on the eight strongest transitions and the resulting spectra added together. Individual gates show coincidences with several other transitions, but at the level of one or two counts in the peaks. Summing the

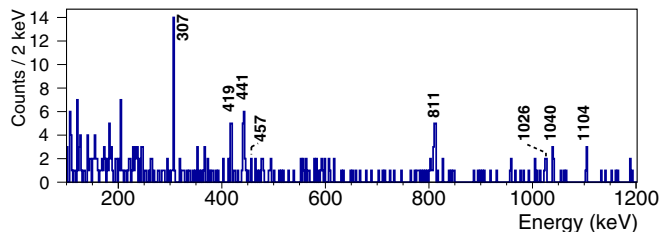


FIG. 3. Sum of projections from a  $\gamma$ - $\gamma$  coincidence matrix from the RIBF83 experiment. Gates were placed on the eight strongest transitions and the resulting spectra were added together.

individually gated spectra produces the expected spectrum showing the eight strongest transitions. This evidence is not unambiguous but does suggest the presence of a cascade of  $\gamma$  rays when combined with the single component to the lifetime fit and the relatively uniform distribution (except the 1561 keV transition) in the  $\gamma$ -ray intensities. The order of the  $\gamma$  rays shown in Fig. 4 is then based on a comparison to shell-model calculations as discussed below.

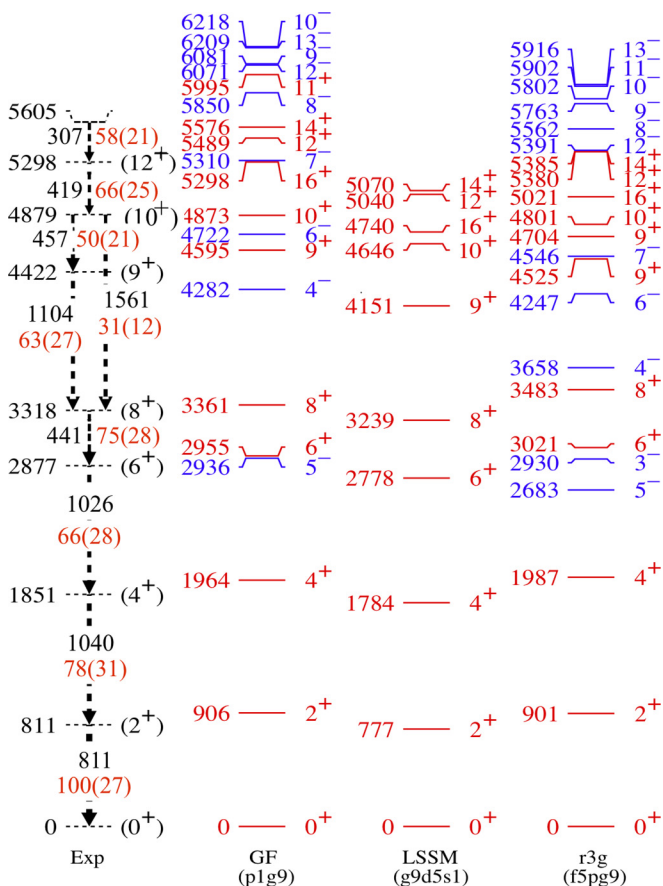


FIG. 4. Tentative energy level scheme (Exp), see text for  $\gamma$ -ray assignments, and SM predictions for calculations performed in the (GF)  $p_{1/2}g_{9/2}$ , (LSSM)  $g_{9/2}d_{5/2}s_{1/2}$ , and (r3g)  $f_{5/2}p_{1/2}g_{9/2}$  model spaces. Calculated positive- and negative-parity states are shown in red and blue, respectively. The % intensities (errors) of the  $\gamma$  rays relative to the 811 keV transition are given in red alongside the energies.

For nuclei around  $^{100}\text{Sn}$  the SM is the tool of choice for understanding nuclear structure. Three of the currently available SM calculations that have been performed using different interactions and model spaces are shown in Fig. 4 (GF, LSSM,  $r3g$ ). These show structural similarities which are employed in the construction of a tentative experimental decay scheme [see Fig. 4 (Exp)]. A detailed discussion of the calculations and the proposed decay scheme is presented below.

In the current work, large-scale shell-model (LSSM) calculations, allowing up to four-particle–four-hole excitations across the  $N = Z = 50$  shell gap, were performed in the  $gds$  model space accounting for positive-parity states only. These are presented in Fig. 4, alongside SM calculations using the Gross-Frenkel (GF) [29] and JUN45 interactions performed in the  $p_{\frac{1}{2}}g_{\frac{3}{2}}$  [17] and  $r3g$  [18] model spaces, respectively. All three model spaces show similar features for the structure of  $^{96}\text{Cd}$ . The relatively even spacing between the  $6^+$ ,  $4^+$ , and  $2^+$  states in these calculations is reminiscent of the low-lying level structure observed in  $^{92}\text{Pd}$ , which was suggested to be a signature of  $T = 0$  spin-aligned  $np$  pairing [3].

Detailed comparison of the observed transitions with the SM calculations strongly suggests that the 811 keV  $\gamma$  ray is the most likely candidate for the decay of the  $2^+$  state, due to the lower transition energy compared to decays from the  $4^+$  and  $6^+$  states and the fact that it appears to have the largest intensity, a feature which may result from the presence of unobserved weak  $\gamma$  rays populating the  $2^+$  state. All of the calculations shown in Fig. 4 predict that the decays from the  $6^+$  and  $4^+$  levels are, to within a few keV, identical; which suggests that the 1026 keV and 1040 keV transitions are the most likely candidates for the decay of these states. The order presented in Fig. 4 is based on the relative energy differences of these states in the various SM calculations, a change in the order of these two  $\gamma$  rays does not affect the conclusions drawn in this paper.

As a result of the differences in model spaces used, and in the case of the LSSM calculations, the truncation level used, we conclude that the calculations show very similar energy spacings for the low-lying positive-parity levels. Indeed, the level of agreement for the decays from the  $2^+$ ,  $4^+$ , and  $6^+$  states suggests that the  $8^+ \rightarrow 6^+$  decay most likely involves the 419 or 441 keV  $\gamma$  rays. We have arbitrarily assumed the latter. A recent theoretical investigation [19] into the pairing approximations that describe the low-lying  $T = 0$  states in  $^{96}\text{Cd}$  revealed that, for  $I < 10$ , no single pair approximation accounted for more than 86% overlap with the SM wave function. The results also indicated that isovector monopole and quadrupole pairing, along with spin-aligned pairing, co-exist in the low-lying states in  $^{96}\text{Cd}$ . Furthermore, for the  $8^+$  state the overlap between the spin-aligned pair approximation and its SM configuration was found to be small, suggesting that the seniority scheme ( $T = 1$  like-nucleon pairing) is at least partially preserved for this state. This is supported by a near identical  $B(E2; 8^+ \rightarrow 6^+)$  extracted from the SM calculations performed for both  $^{96}\text{Cd}$  (present work) and  $^{98}\text{Cd}$  [30]. The conclusion remains valid if any of the transitions

below 500 keV, observed in Fig. 1, represent the  $8^+ \rightarrow 6^+$  decay.

The identification of the tentative transition at 1561 keV leads to a very interesting possibility based on comparison with the SM calculations. The energy gap between the  $T = 0$   $10^+$  and  $8^+$  states suggests that the 1561 keV transition may result from the  $10^+ \rightarrow 8^+$  decay with a parallel decay sequence of 457 keV and 1104 keV  $\gamma$  rays from the  $10^+$  and  $9^+$  states, the ordering of which is unknown (see Fig. 4). In all of the presented SM calculations, the yrast  $9^+$  is found to be a  $T = 1$  state which lies between the  $8^+$  and  $10^+$   $T = 0$  states. In self-conjugate nuclei  $\Delta T = 1$  transitions can produce large  $B(M1)$  values while  $\Delta T = 0$  transitions result in small  $B(M1)$  transition strengths. In the latter case, this results from the fact that in  $T_z = 0$  nuclei the isovector component of the  $M1$  transition matrix element disappears. The dominating isoscalar part, however, is proportional to the destructive  $(g_s^\pi + g_s^\nu)$  value and hence small. Conversely,  $\Delta T = 1$   $M1$  decays are strong as the isovector part depends on  $(g_s^\pi - g_s^\nu)$ . Such strong transitions have been observed in other  $j = l + 1/2$  orbits, for example, the near closed-shell nuclei  $^{18}\text{F}$  and  $^{42}\text{Sc}$  [31]. The scenario discussed above for the three  $\gamma$  rays is consistent with calculations performed with all three SM approaches presented above and which predict branching ratios ranging from 75–90% for the  $M1$   $\gamma$  ray to the yrast  $9^+$  state and 10–25% for the  $E2$  decay to the  $8^+$  state.

The nature of the isomeric state is somewhat puzzling. All of the SM calculations show a  $14^+ \rightarrow 12^+$  transition of 100 keV or below. While it is possible that the  $14^+$  state is isomeric, it is discounted because this scenario would also be expected to result in a  $\gamma$  branch ( $E_\gamma \approx 200$ –300 keV) to the  $\beta$ -decaying  $16^+$  isomeric state with no coincidences to other  $\gamma$  rays and an intensity of the order of 6 or more times greater than the  $14^+ \rightarrow 12^+$  transition. This is based on a conservative estimate which assumes transition energies of 100 and 200 keV for decays to the  $12^+$  and  $16^+$  states, with SM and GF predicted transition strengths of 5 W.u. and 2.5 W.u., respectively. This yields branching ratios of 13% (87%) for the decay to the  $12^+$  ( $16^+$ ) states. The lack of a high-intensity  $\gamma$  ray with energy above 100 keV and no other  $\gamma$  coincidences suggests that the  $14^+$  level is not the observed isomeric state. However, SM calculations in both the  $r3g$  and  $p_{\frac{1}{2}}g_{\frac{3}{2}}$  model spaces show a number of negative-parity states that could be candidates for the isomer. In the case of the 307, 419, and 441 keV transitions the  $B(E1)$ ,  $B(M2)$ , and  $B(E3)$  Weisskopf estimates for a half-life of  $197_{-17}^{+19}$  ns are of the order of  $10^{-8}$ , 1, and  $>1000$  W.u., respectively. The  $B(E3)$  is too large to be realistic and an  $M2$  transition of 1 W.u. is also unlikely as evidenced by experimental upper limits for  $B(M2)$  values of  $<10^{-4}$  W.u. for decays from isomeric transitions in  $^{90}\text{Nb}$  [32,33],  $^{93}\text{Tc}$  [34], and  $^{96}\text{Ag}$  [35]. A retarded  $B(E1)$  is expected for a self-conjugate nucleus and the above value is consistent with the known  $B(E1)$  in  $^{94}\text{Pd}$  which is  $\sim 10^{-7}$  W.u. for the  $19^- \rightarrow 18^+$  transition [36]. Thus, it seems that either  $12^-$  or  $13^-$  are the most likely assignments for the isomer. A  $12^-$  state is predicted to be an odd-parity yrast trap in both the GF and JUN45 ( $r3g$ ) SM calculations (see Fig. 4). This state

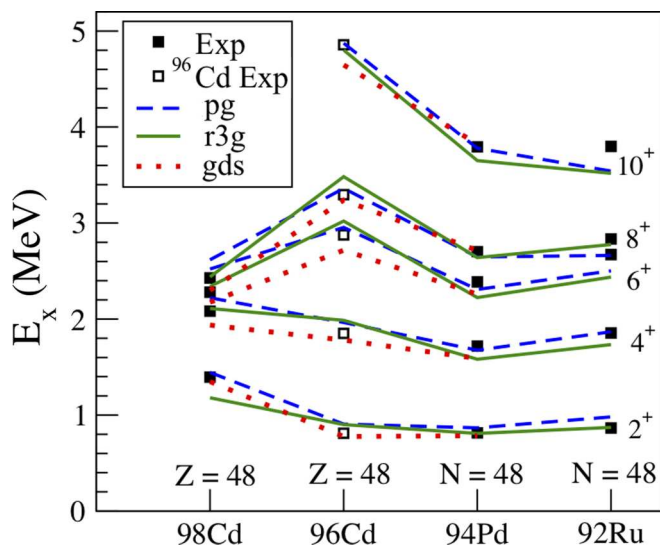


FIG. 5. Experimental (squares) and SM predicted energies of yrast even-spin, positive-parity states for selected isotopes and isotones of  $^{96}\text{Cd}$ ; see text for details. Open squares are used for the tentatively assigned levels in  $^{96}\text{Cd}$ .

may be interpreted in terms of a coupling of the lowest lying  $^{98}\text{In}$   $I^\pi = 4^-$  and  $9^+ T = 0$   $np$  hole pairs, which can yield both  $12^-$  and  $13^-$  states.

Figure 5 shows SM and experimental energy level ( $N, Z = 48$ ) systematics for nuclei bordering  $^{96}\text{Cd}$ , i.e.,  $Z = 48$  Cd isotopes or  $N = 48$  mirror isotones. The energy level spacings suggest that the extra binding in the  $N = Z$  nucleus (resulting from the Wigner term in the ground-state binding energies) is most likely reduced with increasing spin by aligning or breaking of  $np$  pairs. The resulting gaps between groups of states are evident in all three SM calculations shown. Hence, the effect may be ascribed to the  $g_{9/2}$  orbit, which is present, and dominant, in all model spaces.

Recent work by van Isacker [37] discusses  $np$  pairs coupled to  $J^\pi = 9^+$  in terms of B bosons and makes a comparison with SM calculations using the SLGT0 [38] interaction and a simple  $(g_{9/2})^4$  model space. Figure 11 from that work shows the degree of overlap of the yrast eigenstates in the  $(g_{9/2})^4$  SM configuration for angular momentum  $J$  and isospin  $T = 0$  with the B-pair states in  $^{96}\text{Cd}$ . For this nucleus the observed energy gaps at both low and high spins correlate well with the transitional regions where the large overlaps are reduced for intermediate spins and restored toward higher spins.

A further interesting feature is that it is the large energy gap between the  $8^+$  and  $10^+ T = 0$  states in  $^{96}\text{Cd}$  that allows the  $9^+ T = 1$  state to become yrast (Fig. 4). In the  $f_{7/2}$  analog ( $^{52}\text{Fe}$ ) below the doubly closed shell nucleus  $^{56}\text{Ni}$ , the corresponding  $7^+$  state is unknown, but may be inferred from the location of the known  $6^+ T = 1$  level and the  $T = 1$  analog states in  $^{52}\text{Mn}$  to reside above the known  $8^+$  yrast state [39]. This means that the situation in  $^{96}\text{Cd}$  is unique and results in the  $9^+$  state being the lowest known  $T = 1$  yrast state in an even-even  $N = Z$  nucleus. In a pair approximation this state can be viewed as the energetically favored coupling of a  $9^+ (T = 0)$   $np$  pair to a  $0^+ (T = 1)$   $np$  pair, which are the lowest two SM-calculated hole states in  $^{98}\text{In}$ . This indicates that the  $T = 1$  ground-state domination in odd-odd  $N = Z$  nuclei is stronger in the  $g_{9/2}$  shell than in the  $f_{7/2}$  shell.

In summary, a  $\gamma$ -decaying isomer with a half-life of  $197_{-17}^{+19}$  ns has been identified in  $^{96}\text{Cd}$  and nine transitions have been observed following its decay. A tentative decay scheme has been constructed based on comparison with different SM calculations performed in three different model spaces ( $gds$ ,  $pg$ , and  $r3g$ ). Although the ordering of the transitions shown in Fig. 4 may not be unique the excitation energy of the isomeric state is determined to be 5605 keV and some variation in the ordering of the transitions is possible without changing the conclusions of this paper. A detailed comparison of the SM calculations in the  $p_{1/2}, g_{9/2}$ , and  $r3g$  model spaces with the data suggests that the new  $\gamma$ -decaying isomer, with  $J^\pi = 12^-$  or  $13^-$ , can be interpreted as a negative-parity spin-trap state. Both of these states may be interpreted in terms of the coupling of the lowest lying  $^{98}\text{In}$   $I^\pi = 4^-$  and  $9^+ T = 0$   $np$  hole pairs. SM calculations suggest that no single pairing approximation is dominant in the low-lying states, but they imply a reduction in the additional binding energy seen in  $N = Z$  nuclei, leading to groups of states, which is ascribed to the  $g_{9/2}$  orbital. Tentative evidence is presented for the observation of a  $9^+ T = 1$  state. This is the only known  $T = 1$  yrast state in an even-even self-conjugate nucleus.

This work was partially supported by the German BMBF Grants No. 05P12PKFNE and No. 05P15RDFN1, the UK STFC under Grants No. ST/J000124/1 and No. ST/L005727/1, the Natural Sciences and Engineering Research Council (NSERC) of Canada, the U.S. DOE Grant No. DE-FG02-91ER40609, KAKENHI under Grant No. 25247045, and the Spanish Ministerio de Economía y Competitividad under Contract No. FPA2014-57196-C5-4-P.

[1] *Pairing in Fermionic Systems*, Series on Advances in Quantum Many Body Theory, Vol. 8, edited by A. Sedrakian, J. W. Clark, and M. Alford (World Scientific, Singapore, 2006).  
 [2] D. M. Brink and R. A. Broglia, *Nuclear Superfluidity: Pairing in Finite Systems* (Cambridge University, New York, 2005).  
 [3] B. Cederwall, F. G. Moradi, T. Bäck, A. Johnson, J. Blomqvist, E. Clement, G. de France, R. Wadsworth, K. Andgren, K. Lagergren *et al.*, *Nature* **469**, 68 (2011).

[4] A. L. Goodman, *Advances in Nuclear Physics*, edited by J. Negele, Vol. 11 (Plenum Press, New York, 1979), p. 263.  
 [5] A. L. Goodman, *Phys. Rev. C* **63**, 044325 (2001).  
 [6] K. Kaneko, Y. Sun, M. Hasegawa, and T. Mizusaki, *Phys. Rev. C* **77**, 064304 (2008).  
 [7] C. Qi, J. Blomqvist, T. Bäck, B. Cederwall, A. Johnson, R. J. Liotta, and R. Wyss, *Phys. Rev. C* **84**, 021301 (2011).  
 [8] S. Zerguine and P. Van Isacker, *Phys. Rev. C* **83**, 064314 (2011).

- [9] L. Coraggio, A. Covello, A. Gargano, and N. Itaco, *Phys. Rev. C* **85**, 034335 (2012).
- [10] C. B. Hinke, M. Böhmer, P. Boutachkov, T. Faestermann, H. Geissel, J. Gerl, R. Gernhäuser, M. Górska, A. Gottardo, H. Grawe *et al.*, *Nature* **486**, 341 (2012).
- [11] I. Talmi, *Nucl. Phys. A* **172**, 1 (1971).
- [12] I. Talmi, *Nucl. Phys. A* **686**, 217 (2001).
- [13] M. Górska, M. Lipoglavsek, H. Grawe, J. Nyberg, A. Ataç, A. Axelsson, R. Bark, J. Blomqvist, J. Cederkall, B. Cederwall *et al.*, *Phys. Rev. Lett.* **79**, 2415 (1997).
- [14] D. Alber, H. H. Bertschat, H. Grawe, H. Haas, B. Spellmeyer, and X. Sun, *Z. Phys. A - Atomic Nuclei* **335**, 265 (1990).
- [15] W. Kurcewicz, E. F. Zganjar, R. Kirchner, O. Klepper, E. Roeckl, P. Komminos, E. Nolte, D. Schardt, and P. Tidemand-Petersson, *Z. Phys. A* **308**, 21 (1982).
- [16] H. Grawe and H. Haas, *Phys. Lett. B* **120**, 63 (1983).
- [17] B. S. Nara Singh, Z. Liu, R. Wadsworth, H. Grawe, T. S. Brock, P. Boutachkov, N. Braun, A. Blazhev, M. Górska, S. Pietri *et al.*, *Phys. Rev. Lett.* **107**, 172502 (2011).
- [18] A. P. Zuker, A. Poves, F. Nowacki, and S. M. Lenzi, *Phys. Rev. C* **92**, 024320 (2015).
- [19] G. J. Fu, Y. Y. Cheng, Y. M. Zhao, and A. Arima, *Phys. Rev. C* **94**, 024336 (2016).
- [20] S. Frauendorf and A. O. Macchiavelli, *Prog. Part. Nucl. Phys.* **78**, 24 (2014).
- [21] A. V. Afanasjev and S. Frauendorf, *Phys. Rev. C* **71**, 064318 (2005).
- [22] P. J. Davies, H. Grawe, K. Moschner, A. Blazhev, R. Wadsworth, P. Boutachkov, F. Ameil, A. Yagi, H. Baba, T. Bäck *et al.*, *Phys. Lett. B* **767**, 474 (2017).
- [23] T. Kubo, D. Kameda, H. Suzuki, N. Fukuda, H. Takeda, Y. Yanagisawa, M. Ohtake, K. Kusaka, K. Yoshida, N. Inabe *et al.*, *Prog. Theor. Exp. Phys.* **2012**, 03C003 (2012).
- [24] T. Kubo, *Nucl. Instrum. Meth. B* **204**, 97 (2003).
- [25] P. A. Söderström, S. Nishimura, P. Doornenbal, G. Lorusso, T. Sumikama, H. Watanabe, Z. Y. Xu, H. Baba, F. Browne, S. Go *et al.*, *Nucl. Instrum. Meth. B* **317**, 649 (2013).
- [26] I. Čeliković, M. Lewitowicz, R. Gernhäuser, R. Krücken, S. Nishimura, H. Sakurai, D. S. Ahn, H. Baba, B. Blank, A. Blazhev *et al.*, *Phys. Rev. Lett.* **116**, 162501 (2016).
- [27] K. H. Schmidt, C. C. Sahm, K. Pielenz, and H. G. Clerc, *Z. Phys. A* **316**, 19 (1984).
- [28] R. Barlow, [arXiv:physics/0403046v1](https://arxiv.org/abs/physics/0403046v1).
- [29] R. Gross and A. Frenkel, *Nucl. Phys. A* **267**, 85 (1976).
- [30] A. Blazhev, M. Górska, H. Grawe, J. Nyberg, M. Palacz, E. Caurier, O. Dorvaux, A. Gadea, F. Nowacki, C. Andreoiu *et al.*, *Phys. Rev. C* **69**, 064304 (2004).
- [31] A. F. Lisetskiy, R. V. Jolos, N. Pietralla, and P. von Brentano, *Phys. Rev. C* **60**, 064310 (1999).
- [32] C. A. Fields, F. W. N. De Boer, J. J. Kraushaar, R. A. Ristinen, L. E. Samuelson, and E. Sugarbaker, *Nucl. Phys. A* **363**, 311 (1981).
- [33] O. Häusser, T. Faestermann, I. S. Towner, T. K. Alexander, H. R. Andrews, J. R. Beene, D. Horn, D. Ward, and C. Broude, *Hyperfine Interact.* **4**, 196 (1978).
- [34] B. A. Brown, D. B. Fossan, P. M. S. Lesser, and A. R. Poletti, *Phys. Rev. C* **13**, 1194 (1976).
- [35] P. Boutachkov, M. Górska, H. Grawe, A. Blazhev, N. Braun, T. S. Brock, Z. Liu, B. S. Nara Singh, R. Wadsworth, S. Pietri *et al.*, *Phys. Rev. C* **84**, 044311 (2011).
- [36] T. S. Brock, B. S. Nara Singh, P. Boutachkov, N. Braun, A. Blazhev, Z. Liu, R. Wadsworth, M. Górska, H. Grawe, S. Pietri *et al.*, *Phys. Rev. C* **82**, 061309 (2010).
- [37] P. Van Isacker, *Int. J. Mod. Phys. E* **22**, 1330028 (2013).
- [38] F. J. D. Serduke, R. D. Lawson, and D. H. Gloeckner, *Nucl. Phys. A* **256**, 45 (1976).
- [39] Evaluated Nuclear Structure Data File (2017), <http://www.nndc.bnl.gov/ensdf>.